Accepted Manuscript

Radiological Evaluation of Maxillary Sinus Anatomy: A cross-sectional study of 300 Patients

Running title: Cone beam sinus anatomy

Naroa Lozano-Carrascal[a], Oscar Salomó-Coll[b], Sergio Alexandre Gehrke[c], José Luis Calvo-Guirado[d], Federico Hernández-Alfaro[e], Jordi Gargallo-Albiol[f].

[a]Clinical Instructor of the International Master in Oral Surgery (IMOS). International University of Catalonia (UIC), Barcelona, Spain.

[b]Assistant Professor of the International Master in Oral Surgery (IMOS). International University of Catalonia (UIC), Barcelona, Spain.

[c]Professor and Director of Biotechnology Cathedra, San Antonio Catholic University of Murcia (UCAM), Murcia, Spain.

[d]Full Professor and Director of International Dentistry Research Cathedra, Faculty of Medicine & Dentistry, San Antonio Catholic University of Murcia (UCAM), Murcia, Spain.

[e]Professor and Chairman of the Department of Oral and Maxillofacial Surgery, International University of Catalonia (UIC), Barcelona, Spain

[f]Director and Associate Professor of the International Master in Oral Surgery (IMOS), International University of Catalonia (UIC), Barcelona, Spain.

Corresponding author:

Oscar Salomó-Coll

Faculty of Medicine and Dentistry, Universitat Internacional de Catalunya

Carrer de Josep Trueta s/n

08195 Sant Cugat del Vallés

Barcelona, Spain

e-mail: oscarsalomo@uic.es

ABSTRACT

Objective: The aim of the present study was to evaluate the principal anatomical characteristics of the maxillary sinus using Cone Beam Computed Tomography (CBCT) in order to facilitate prevention of intra- and post-operative complications.

Materials and methods: Three hundred CBCT scans from patients undergoing implant surgery were analysed. The following anatomical structures were evaluated: (1) Residual ridge height (RRH) and width (RRW); (2) Ridge bone density (BD); (3) Maxillary sinus angle (MSA); (4) Maxillary sinus lateral wall thickness (LWT); (5) Schneiderian membrane thickness (MT); (6) Maxillary sinus septa (SS); (7) Posterior superior alveolar artery (PSAA).

Results: Mean patient age was 59.5±13.6. Mean RRH at upper second premolar (2PM) was 8.66±3.95 mm, 4.90±2.28 mm at first molar (1M), and 5.26±2.13 mm at second molar (2M). Mean RRW was 6.72±2.69 mm at 2PM , 6.87±2.65 mm at 1M and 7.09±2.80 mm at 2M. Bone Density was 330.93±211.02 Hounsfield Units (HU) at first molar position and MSA was 73.39±15.23º. LWT was 1.95±0.98 mm. Mean Schneider Membrane thickness (MT) was 1.82±1.59 mm; MT was ≤ 3mm in 72.9% of patients and >3mm in 27.10%. 20.56% of patients presented bucco-palatal oriented septa with a mean height of 13.11±3.82 mm. PSAA was observed in 48.60% and mean distance to the top of the ridge was 13.15±3.71 mm, and was mostly observed inside the sinus (53.85%).

Conclusions: CBCT scanning has been shown to be a useful tool for evaluating maxillary sinus anatomical variations. CBCT should be considered the gold standard when evaluating the maxillary sinus area.

Keywords: maxillary sinus, cone beam computed tomography, CBCT, sinus anatomy, sinus abnormalities.

INTRODUCTION

Dental extraction and the progressive pneumatization of the maxillary sinus can create difficulties when it comes to the placement of dental implants in the upper posterior region. In cases of severe atrophy, sinus lift with lateral approach remains the gold standard when implants are to be placed. Maxillary sinus floor elevation is a reliable technique associated with high implant survival rate but the procedure does run a risk of complications (Del Fabbro et al., 2008; Katranji et al., 2008; Tan et al., 2008; Esposito et al., 2010). The most common intra-operative complication is perforation of the sinus membrane (19.5%), but other complications such as excessive bleeding, hematoma, or wound dehiscence also occur (Pjetursson *et al.* 2008). Given this situation, the anatomy of the area should be carefully examined before any surgical intervention. Accurate diagnosis of antral anatomy may avoid or prevent many potential complications.

The maxillary sinus may exhibit a number of anatomic variations such as ~~pneumatization~~ hypoplasia, antral septa, or bone exostosis. Maxillary sinus lesions are also fairly common; these include mucosal thickening, sinusitis, mucus retention cyst, discontinuity of the sinus floor, polypoid lesions, discontinuity of the sinus lateral wall, or foreign bodies (Lana et al., 2011). The most widely studied anatomical structure is the maxillary septum, the anatomy of which may complicate the creation and removal of the access window during lateral sinus floor elevation (Betts & Miloro, 1994). As a result, this anatomical variation is often associated with sinus membrane perforation (Ardekian et al., 2006; Becker et al., 2008; Hernádez-Alfaro et al., 2008). Knowledge of the location and morphology of the sinus septa is essential to determining the best surgical approach (Ulm et al., 1995; Krenmair et al., 1997; Zijderveld et al., 2008; Wen et al., 2013). When performing ~~the~~ lateral window osteotomy, it not uncommon to cut the blood supply, compromising vascular supply, which results in excessive intraoperative bleeding (Ella et al., 2008). The dental branch of the posterior superior alveolar artery (PSAA) and infraorbital artery (IOA) supply the lateral sinus wall and overlying membrane; it is not uncommon to find an intra-osseous anastomosis between the PSAA and IOA (Rosano et al., 2011). The PSAA runs caudally on the outside of the

convexity of the maxillary tuberosity, in close contact with bone and periosteum (Solar et al., 1999; Traxler et al., 1999).

During the 20th century, the diagnostic tools in implant dentistry consisted of clinical examination, and two-dimensional (2D) imaging (Harris et al., 2002; Bornstein et al., 2014). The information provided by these tools was incomplete and often poor in quality. To overcome the limitations of these techniques, 3D projections, know as computed tomography (CT), were introduced (Hounsfield, 1980) providing more complete information than conventional two-dimensional x-rays. However, this technique suffered the disadvantage of exposing the patient to high doses of radiation. Later on, cone beam computed tomography (CBCT) was developed. This radiological exploration technique applies a conical- or pyramidal- shaped beam to acquire multiple projections in a single rotation (Koong, 2010). CBCT creates a 3D view at a lower level of radiation exposure and a higher diagnostic capability. Since it was first described by Mozzo *et al*. 1998 CBCT has become an essential diagnostic tool, with many applications in implant dentistry, both in terms of the surgery itself and for bone quality assessment (Harris et al., 2012).

Previous studies have investigated the anatomy of maxillary sinus by observation of anatomic cadavers, intra-operatively during surgical procedures, by computed tomography (CT) or by use of panoramic x-rays (2D) (Neugebauer et al., 2010), but most studies have only considered one anatomical structure at a time.

For this reason, the aim of this study has been to assess the normal anatomy and prevalence of anatomical variations of the main maxillary sinus structures by means of CBCT scan analysis.

MATERIAL AND METHODS

Study design

Three hundred consecutive CBCT scans of Caucasian adult patients with maxillary posterior atrophy were used to perform the study. The CBCT scans were obtained from patients attending the Dental Clinic at the International University of Catalonia (Spain) (*Clinica Odontológica*

Universitaria de la Universitat Internacional de Catalunya) between January 2008 and April 2015, requiring rehabilitation with dental implants. Established clinical practice based on the International Master in Oral Surgery includes a CBCT scan captured for purposes of diagnosis and implant planning, so patients did not received any extra exposure to radiation as a result of taking part in the study. The study was approved by the Ethics Committee for Research of the International University of Catalonia (Spain) (CIR-ECL-2014-05).

The following inclusion criteria were applied: (1) Existence of CBCT scan of the maxilla; (2) CBCT scan performed using a radiological guide (Fig. 1); (3) edentulism of at least one upper molar; and (4) less than 8 mm of distance between the residual ridge and the sinus floor in the molar area. CBCT explorations that did not fulfil these inclusion criteria, or images that were unclear or incomplete were rejected. In cases in which both hemi-maxillas were available for analysis only one side of the maxilla was used, which was selected by following a randomization scheme generated using the web site http:// www.randomizer.com.

The same radiological operator performed all examination procedures. An i-CAT cone beam computed tomography scanner (CBCT) (Kavo Dental GmbH®, Biberoch, Germany) was used with a flat panel detector. Exposure volume was set at 102 mm diameter and 102 mm height; the voxel size was 0.2 mm x 0.2 mm x 0.2 mm; the exposure volume was set at 0.4 mm; and the scan was set at 80 kV and 5 mA, as recommended by the manufacturer. The Frankfort horizontal plane was used as a reference to standardize CBCT scans, as this remains stable in patients with posterior edentulism.

Image analysis

Two independent observers examined the CBCT scans. Image analysis was performed using i-CAT software (I-CATVision®, Kavo Dental GmbH, Biberoch, Germany) and a multiplanar reconstruction window whereby the axial, coronal and sagittal planes could be visualized in 0.3 mm intervals. Measurements were made by the digital ruler included in the software. The observers were free to adjust the orientation, brightness and contrast of the CBCT images to facilitate image analysis.

The following maxillary sinus anatomical structures and variations were assessed: (1) Residual ridge height (RRH) and width (RRW); (2) Ridge bone density (BD); (3) Maxillary sinus angle (MSA); (4) Maxillary sinus lateral wall thickness (LWT); (5) Schneiderian membrane thickness (MT); (6) Maxillary sinus septa (SS); and (7) Posterior superior alveolar artery (PSAA).

Residual ridge (RR)

Residual ridge height (RRH) was measured in millimetres (mm) between the most coronal point of the alveolar crest and the sinus floor at three positions: second premolar (2PM); first molar (1M); second molar (2M).

Residual ridge width (RRW) was measured in millimetres (mm) at the top of the residual ridge, measuring from the palatal to buccal aspect, perpendicular to the vertical measurements taken at three positions: second premolar (2PM); first molar (1M); second molar (2M). Linear measurements were taken from sagittal images ~~were radiological marks were seen~~. All measurements were taken in edentulous areas (Fig. 2).

Bone density (BD)

Establishing a 3 mm^2 area, Hounsfield unit evaluation (HU) was registered in the first molar region at the centre of the residual ridge; bone density was calculated using i-CAT software (I-CATVision® Software).

Maxillary sinus angle (MSA)

The angle between the inner and outer walls of the sinus was calculated in the first molar region (Fig.2). To measure the distance between the two walls, a horizontal line was drawn 10 mm from the base of the sinus, simulating the top of the augmented area. The sinus angle was calculated according to the function (SA = 2α   α=-1TANα   Tanα = ½ W/ 10).

Lateral wall thickness (LWT)

The thickness of the lateral wall was measured four millimetres from the lowest point of the sinus floor in the first molar region, simulating the lower part of the lateral window access during a sinus augmentation procedure. Measurements were performed parallel to the residual ridge and registered in millimetres.

Schneiderian membrane thickness (MT)

Membrane Thickness was measured in millimetres in the first molar region perpendicular to the underlying bone at the base of the sinus. The mean ~~value~~ was recorded and categorized as two groups: (1) ≤ 3mm ('Normal') or (2) > 3mm ('Pathological') (White & Pharoah, 2004).

Maxillary sinus septa (SS)

Septa were analysed using three orthogonal slice views: axial, coronal and sagittal. Each septum was classified according to its orientation into three groups: transversal (bucco-palatal), sagittal (mesio-distal), or horizontal (parallel to the sinus floor) (Pommer *et al*., 2012). Each septum was measured in millimetres from the top of the septum to the coronal part of the residual ridge, registering the measurement at the highest point on the septum.

Posterior Superior Alveolar Artery (PSAA)

PSAA evaluation was performed in the axial sections where the artery was first visualized moving from mesial to distal. The distance between the lower borders of the artery perpendicular to the alveolar crest was measured in millimetres (Elian et al., 2005) (Fig. 3). The diameter of the artery

was categorized as one of three groups: (1) <1 mm; (2) 1 - 2 mm; and (3) >2 mm (Mardinger et al., 2007). The position of the artery was divided into one of three categories: (1) intraosseous; (2) below the membrane; (3) at the outer cortex of the lateral sinus wall (Güncü et al., 2011).

Statistical Analysis

Data were entered on a Microsoft Excel Office® 2011 spreadsheet (Microsoft Corporation, Redmond, USA). Statistical analysis was performed using Statgraphics® Plus 5.1 software (Statpoint Technologies, INC Virginia, USA). The mean ~~value~~ and standard deviation of the different continuous variables was calculated. For qualitative variables, frequency was determined. Intraobserver agreement ~~degree~~ was calculated using the Kappa-Index for qualitative measurements. In case of quantitative variables, multifactorial ANOVA for repeated measurements ~~test~~ was applied. A p value of less than 0.05 was considered indicative of statistical significance.

RESULTS

A total of 284 scans were included for analysis, 16 having been were rejected because of low quality images, evidence of previous implant placement and/or augmentation procedures. Of the 284 evaluated CBCTs, 54% belonged to female patients and 46% to males. Mean age in both groups was 59.5 ± 13.6.

Mean residual ridge height (RRH) in the position of the upper second premolar (2PM) was 8.66±3.95 mm; 4.90±2.28 mm at the first molar (1M); and 5.26±2.13 mm at the second molar (2M). Mean residual ridge width (RRW) at 2PM was 6.72±2.69 mm; 6.87±2.65 mm at M1; and 7.09±2.80 mm at 2M; (p>0.05). In the first molar region, mean bone density (BD) was 330.93±211.02 HU (p>0.05); mean maxillary sinus angle (MSA) was 73.39± 15.23º (p>0.05) (Table 1).

Mean thickness of the maxillary sinus lateral wall (LWT) in the position of the first molar was 1.95±0.98, (p>.05). Mean thickness of the Schneiderian Membrane (MT) in the first molar region

was 1.82 ± 1.59 mm (p >.05). MT was ≤ 3mm in 72.9% of the patients and >3mm in 27.10% of cases. Perfect agreement was reached between the two examiners (K=0.928, Very Good) (Table 2).

Septa with bucco-palatal orientation were observed in 20.56% of patients (K=0.638, Good) (Fig.4). The mean height of these septa, measured from the top of the septum to the alveolar crest, was 13.11±3.82 mm (p >.05), and were mostly found in the second molar region (40.91%), followed by the third molar (22.73%), the first molar region (22.73%), and the second premolar (13.64%) (K=0.833, Very Good). For sagittal septa, prevalence was 3.74% (K=-0.039, Poor) (Fig. 5). Mean height of sagittal septa was 12.24±1.25 mm and the most common position was in the second premolar region (50%), followed by the first molar (25%) and third molar (25%). No sagittal septum was found in the second molar position. No septum with horizontal orientation was found in any of the CBCTs studied (Table 3).

The posterior superior alveolar artery (PSAA) was observed radiographically in 48.60% of the sinuses assessed, with good intraobserver agreement ~~reached~~ (K=0.682, Good). The mean distance between the lower border of the artery and the alveolar crest was 13.15±3.71 mm (p>0.05), and was mostly observed inside the sinus below the Schneiderian membrane (53.85% of cases), intraosseous in 38.46% of cases (Fig. 6), and located in the outer cortex of the lateral sinus wall in 7.69% of cases, with moderate agreement between the observers (K=0.404, Moderate). The most common position at which the artery was first visualized was the first molar area (46.15%). Regarding PSAA diameter, in 36.54% of the sinus studied, was < 1 mm, in 28.85% mm was between 1 and 2 millimetres, and 34.62% was > 2 mm, although weak intraobserver agreement was reached for these two variables. All the above results were obtained by the first observer (Table 4).

DISCUSSION

Sinus augmentation has become a very reliable technique, although it may suffer complications. However, many of these undesirable complications – which can compromise long-term outcomes – can be avoided by prior knowledge of the maxillary sinus anatomic structures.

The present study of the maxillary sinus using CBCT scans, obtained a mean residual ridge height (RRH) that concurred with Shanbhag et al. (2014). These authors found that most patients presented a residual ridge > 8mm in the 2nd PM region, and ≥ 4mm in the 1st M and 2nd M regions.

Hounsfield units (HU) permit bone density assessment on the basis of computed tomography. Bone density usually ranges between 50 and 2,500 HU. In the present study, mean bone density in the 1st M region was 330.93±211.02 HU (range, 72-1,055 HU), presenting values that correspond to the fine trabecular bone usually found in the posterior maxilla (Misch & Kircos, 1999). A maximum value of 1,055 HU was measured in patients with severe posterior atrophy, where the residual ridge was mostly cortical bone.

We have been unable to locate any literature dealing with sinus angle (SA). However, according to our understanding, the closer the sinus walls are, the greater the blood supply to the grafted area will be, a fact that could accelerate graft integration.

In a cadaver study carried out by Yang et al. (2009), mean thickness of the lateral wall (LWT) in the first molar region ranged between 1.54±0.89 mm and 1.45±0.79 depending on the vertical height where the LWT was measured. The values obtained in the present study for the LWT, measured at 4 mm height from the sinus floor in the 1st M region, were similar to those obtained by Yang et al. (2012), who reported mean LWT in the 1st M region of 1.77±0.78, measured from CBCT scans. However, data should be treated with caution due to the differences in methodology between the present study and the former one and to the fact that chronic inflammation may have affected maxillary sinus wall thickness (Deeb *et al*. 2011).

The percentage of pathological MT in the present study was lower than reported by Lana et al. (2011), who obtained MT >3mm in 62.6% of cases. For Shanbhag et al. (2014), MT >2 mm was considered pathological in their study of 128 patients, which found that 60.6% of patients presented

pathological membranes. These variations in the thickness criterion deemed pathological could lead to under/overestimating the number of cases presenting pathological membrane thickening. Pathological MT could be a risk affecting post-operative development of maxillary sinusitis (Manor et al., 2010). One limitation in the present study was the absence of clinical data regarding any previous history of sinusitis. Future research should assess the relationship between pathological MT and sinus pathology. In addition, a clear definition of pathological sinus membrane needs to be established.

In previous research, the prevalence of maxillary sinus septa reported using 3D radiological systems ranges between 20.45% (Shen *et al*. 2012) and 66.7% (Maestre-Ferrin *et al*. 2011). A systematic review carried out by Pommer *et al*. 2012 included 8,923 maxillary sinuses, finding a prevalence of septa of 28.4%. Most studies are in agreement with the results reported by Pommer et al. (2012) that the prevalence of maxillary sinus septa is around 28%, that most present transversal (bucco-palatal) orientation, and are found in the molar region, especially in the region of the 1st and 2[nd]M (Kim et al., 2006; Neugebauer et al., 2010; Pommer et al., 2012). In a study ~~performed~~ by Jang *et al*. (2012) on 100 randomly selected patients, no sagittal septa were found among dentulous patients, and only one septum among edentulous patients. Neugebauer *et al*. 2010 examined 1,029 CBCT scans and 2,058 sinuses, obtaining a mean height for transversal septa of 7.3±5.08 mm. In the present study, mean transversal septa height was greater, probably because measurements were made from the top of the septa to the alveolar ridge, instead of the maxillary sinus floor. In our opinion, measurements taken from the top of the ridge are more accurate than those measured from the sinus floor because the location, number, orientation and size of the septa influence the design and creation of the lateral window (Wen et al., 2013). Only septa higher than 4 mm should be taken into consideration in order to exclude irregularities in sinus anatomy (Ulm et al., 1995).

Regarding horizontally orientated septa, the Kappa index obtained poor inter-examiner agreement, with examiners achieving visualizations in different patients. Due to the difficulties of interpretation of septa-related variables, they should only be assessed by experienced examiners.

In reference to the PSSA, previous studies have reported a widely varying prevalence of radiographic artery visualization: 89.3% (Ilgüy et al., 2013); 64.5% (Güncü et al., 2011); 55% (Mardinger et al., 2007); or 52% (Kim et al., 2011). In the present study, the artery was visualized in 48.60% of cases, with good intra-observer agreement. Other studies on larger samples (Elian et al., 2005; Mardinger et al., 2007; Kim et al., 2011) have reported lower percentages of artery visualization. Differences between these results could be due to differences in method.

For Güncü et al. (2011), the mean distance between the lower border of the artery and the alveolar crest was 18±4.9 mm, while in the present study this distance was shorter, with perfect agreement between the two examiners. These differences in mean values could be explained by the differences in residual crestal ridge dimensions; moreover, the standard deviations found were very similar. In a study by Güncü et al. (2011), the mean vertical ridge dimension was 10.2±4.8 mm, while in the present study this distance was considerably lower. Kim *et al*. 2011 concurred with the present results, observing a mean distance between the lower border of the artery and the alveolar crest of 18.9±4.21 mm in the premolar area, while in the molar area they obtained 15.45±4.04 mm. The height of the residual bone ridge appears to play a significant role in the location of the artery, the lower the mean ridge height, the less mean distance (Mardinger et al., 2007).

Moderate intraobserver agreement was obtained regarding PSAA position. For the first examiner, this was mostly below the Scheniderian membrane , and for the second examiner it was mostly intraosseous . The two examiners agreed that the most infrequently visualized position was in the outer cortex of the lateral wall. In studies carried out by Güncü et al. (2011) and Ilgüy et al. (2013), the artery was most frequently detected in an intraosseous position, followed by a position below the membrane. These differences may be explained by the anatomic variations in the position where the artery was first seen.

Regarding PSSA diameter, in the present study artery diameters were mostly ≤ 1mm. These results agree with Elian et al. (2005) and Ilgüy et al. (2013), who found that of 135 CBCT scans analysed, the artery diameter was ≤ 1mm in 68.9% of cases. However, Güncü et al. (2011), Ella et al. (2008)

and Kim et al. (2011) reported higher PSSA diameters of between 1 and 2 mm. In patients with an artery diameter of 1-2 mm, the probability of haemorrhage is about 57% (Ella et al., 2008). In the present study, the examiners visualized the artery in the same patients, achieving perfect intra-observer agreement for the prevalence and the mean distance between the lower border of the artery and the alveolar crest; but no agreement was obtained between the observers as to the position at which the artery was first observed.

CONCLUSIONS

CBCT scans are a useful tool for evaluating maxillary sinus anatomy, especially for evaluating the sinus membrane, mucosa thickening, bone density, position of the superior alveolar artery, and sinus septum. The high percentages of variation found among patients stress the need to perform CBCT studies routinely prior to any surgery located close to the maxillary sinus area.

Conflict of interest

The authors declare that they have no conflict of interest.

Ethical approval

Approved by the Ethics Committee for Research of the International University of Catalonia (Spain), (CIR-ECL-2014-05).

REFERENCES

Ardekian, L., Oved-Peleg, E., Mactei, E.E., Peled, M., 2006. The clinical significance of sinus membrane perforation during augmentation of the maxillary sinus. J Oral Maxillofac Surg. 64, 277–282.

Becker, S.T., Terheyden, H., Steinriede, A., Behrens, E., Springer, I.,Wiltfang, J., 2008. Prospective observation of 41 perforations of the Schneiderian membrane during sinus floor elevation. Clin Oral Implants Res. 19, 1285–1289.

Betts, N.J., Miloro, M., 1994. Modification of the sinus lift procedure for septa in the maxillary antrum. J Oral Maxillofac Surg. 52, 332–343.

Bornstein, M.M., Scarfe, W.C., Vaughn, V.M., Jacobs, R., 2014. Cone beam computed tomography in implant dentistry: A systematic review focusing on guidelines, indications, and radiation dose risks. Int J Oral Maxillofac Implants. 29, 55-77.

Chiapasco, M., Zaniboni, M., Rimondini, L., 2008. Dental implants placed in grafted maxillary sinuses: a retrospective analysis of clinical outcome according to initial clinical situation and a proposal of defect classification. Clin Oral Implants Res. 19, 416–428.

Deeb, R., Malani, P.N., Gil, B., Jafari-Khouzani, K., Soltanian-Zadeh, H., Patel, S., Zacharek, M.A., 2011. Three-dimensional volumetric measurements and analysis of the maxillary sinus. Am J Rhinol Allergy. 25, 152-156.

Del Fabbro, M., Rosano, G., Taschieri, S., 2008. Implant survival rates after maxillary sinus augmentation. Eur J Oral Sci. 116, 497–506.

Elian, N.,Wallace, S., Cho, S.C., Jalbout, Z.N., Froum, S., 2005. Distribution of the maxillary artery as it relates to sinus floor augmentation. Int J Oral Maxillofac Implants. 20, 784–787.

Ella, B., Sedarat, C., Noble Rda, C., Normand, E., Lauverjat, Y., Siberchicot, F., Caix, P., Zwetyenga, N., 2008. Vascular connections of the lateral wall of the sinus: surgical effect in sinus augmentation. Int J Oral Maxillofac Implants. 23, 1047–1052.

Esposito, M., Grusovin, M.G., Rees, J., Karasoulos, D., Felice, P., Alissa, R., Worthington, H., Coulthard, P., 2010. Effectiveness of sinus lift procedures for dental implant rehabilitation: a Cochrane systematic review. Eur J Oral Implantol. 3, 7-26.

Güncü, G. N., Yildirim, Y. D., Wang, H. L., Tözüm, T. F., 2011. Location of posterior superior alveolar artery and evaluation of maxillary sinus anatomy with computerized tomography: a clinical study. Clin Oral Implants Res. 22, 1164–1167.

Harris, D., Buser, D., Dula, K., Grondahl, K., Harris, D., Jacobs, R., Lekholm, U., Nakielny, R., Van Steenberghe, D., Van der Stelt, P., 2002. E.A.O. Guidelines for the use of Diagnostic Imaging in Implant Dentistry. Clin Oral Implants Res. 13, 566-570.

Harris, D., Horner, K., Grondahl, K., Jacobs, R., Helmrot, E., Benic, G.I., Bornstein, M.M., Dawood, A., Quirynen, M., 2012. E.A.O. guidelines for the use of diagnostic imaging in implant dentistry 2011. A consensus workshop organized by the European Association for Osseointegration at the Medical University of Warsaw. Clini Oral Implants Res. 23, 1243–1253.

Hernandez-Alfaro, F., Torradeflot, M.M., Marti, C., 2008. Prevalence and management of Schneiderian membrane perforations during sinus-lift procedures. Clin Oral Implants Res. 19, 91–98.

Hounsfield, G.N., 1980. Nobel Award address. Computed medical imaging. Med Phys. 7, 283-290.

Ilgüy, D., Ilgüy, M., Dolekoglu, S., Fisekcioglu, E., 2013. Evaluation of the posterior superior alveolar artery and the maxillary sinus with CBCT. Braz Oral Res. 27, 431-437.

Jang, S.Y., Chung, K., Jung, S. Park, H.J., Oh, H.K., Kook, M.S., 2014. Comparative study of the sinus septa between dentulous and edentulous patients by cone beam computed tomography. Implant Dent. 23, 477-481.

Katranji, A., Fotek, P., Wang, H.L., 2008. Sinus augmentation complications: Etiology and treatment. Implant Dent. 17, 339–49.

Kim, J.H., Ryu, J.S., Kim, K.D., Hwang, S.H., Moon, H.S., 2011. A radiographic study of the posterior superior alveolar artery. Implant Dent. 20, 306-310.

Kim, M. J., Jung, U. W., Kim, C. S., Kim, K. D., Choi, S. H., Kim, C. K., Cho, K. S., 2006. Maxillary sinus septa: prevalence, height, location, and morphology. A reformatted computed tomography scan analysis. J Periodontol. 77, 903–908.

Koong, B., 2010. Cone beam imaging: is this the ultimate imaging modality? Clin Oral Implants Res. 11, 1201–1208.

Krennmair, G., Ulm, C., Lugmayr, H., 1997. Maxillary sinus septa: Incidence, morphology and clinical implications. J Craniomaxillofac Surg. 25, 261–265.

Maestre-Ferrín, L., Carrillo-García, C., Galán- Gil, S., Peñarrocha-Diago, M., Peñarrocha- Diago, M., 2011. Prevalence, location, and size of maxillary sinus septa: panoramic radiograph versus computed tomography scan. J Oral Maxillofac Surg. 69, 507–511.

Manor, Y., Mardinger, O., Bietlitum, I., Nashef, A., Nissan, J., Chaushu, G., 2010. Late signs and symptoms of maxillary sinusitis after sinus augmentation. Oral Surg Oral Med Oral Pathol Oral Radiol Endod. 110, 1-4.

Mardinger, O., Abba, M., Hirshberg, A., Schwartz-Arad, D., 2007. Prevalence, diameter and course of the maxillary intraosseous vascular canal with relation to sinus augmentation procedure: a radiographic study. Int J Oral Maxillofac Surg. 36, 735–738.

Misch, C.E., Kircos, L.T., 1999. Diagnostic imaging and techniques. Contemporary implant dentistry, 2th edition, 73-87, St Louis, Mosby.

Mozzo, P., Procacci, C., Tacconi, A., Tinazzi Martini, P., Bergamo Andreis, .IA., 1998. A new volumetric CT machine for dental imaging based on the cone-beam technique: Preliminary results. Eur Radiol. 8, 1558-1564.

Neugebauer, J., Ritter, L., Mischkowski, R. A., Dreiseidler, T., Scherer, P., Ketterle, M., Rothamel, D., Zöller, J. E., 2010. Evaluation of maxillary sinus anatomy by cone-beam CT prior to sinus floor elevation. Int J Oral Maxillofac Implants. 25, 258–265.

Park, Y. B., Jeon, H. S., Shim, J. S., Lee, K. W., Moon, H. S., 2011. Analysis of the anatomy of the maxillary sinus septum using 3-dimensional computed tomography. J Oral Maxillofac Surg. 69, 1070–1078.

Pelinsari Lana, J., Moura Rodrigues Carneiro, P., de Carvalho Machado, V., Eduardo Alencar de Souza, P., Ricardo Manzi, F., Campolina Rebello Horta, M., 2011. Anatomic variations and lesions of the maxillary sinus detected in cone beam computed tomography for dental implants. Clin Oral Implants Res. 23, 1398-1403.

Pjetursson, B.E., Tan, W.C., Zwahlen, M., Lang, N.P., 2008. A systematic review of the success of sinus floor elevation and survival of implants inserted in combination with sinus floor elevation. Part I: Lateral approach. J Clin Periodontol. 35, 216–240.

Pommer, B., Ulm, C., Lorenzoni, M., Palmer, R., Watzek, G., Zechner, W., 2012. Prevalence, location and morphology of maxillary sinus septa: systematic review and meta-analysis. J Clin Periodontol. 39, 769-773.

Rosano, G., Taschieri, S., Gaudy, J.F., Del Fabbro, M., 2009. Maxillary sinus vascularization: a cadaveric study. J Craniofac Surg. 20, 940–943.

Shanbhag, S., Karnik, P., Shirke, P., Shanbhag, V., 2014. Cone-beam computed tomographic analysis of sinus membrane thickness, ostium patency, and residual ridge heights in the posterior maxilla: implications for sinus floor elevation. Clin Oral Implants Res. 25, 755-760.

Shen, E. C., Fu, E., Chiu, T. J., Chang, V., Chiang, C. Y., Tu, H. P., 2012. Prevalence and location of maxillary sinus septa in the Taiwanese population and relationship to the absence of molars. Clin Oral Implants Res. 23, 741-745.

Solar, P., Geyerhofer, U., Traxler, H., Windisch, A., Ulm, C., Watzek, G., 1999. Blood supply to the maxillary sinus relevant to sinus floor elevation procedures. Clin Oral Implants Res. 10, 34–44.

Tan, W.C., Lang, N.P., Zwahlen, M., Pjetursson, B.E., 2008. A systematic review of the success of sinus floor elevation and survival of implants inserted in combination with sinus floor elevation. Part II: Transalveolar technique. J Clin Periodontol. 35, 241–254.

Tatum, H., 1986. Maxillary and sinus implant reconstruction. Dent Clin North Am. 30, 207–229.

Traxler, H., Windisch, A., Geyerhofer, U., Surd, R., Solar, P., Firbas, W., 1999. Arterial blood supply of the maxillary sinus. Clin Anat. 12, 417– 421.

Ulm, C., Solar, P., Krennmair, G., Matejka, M., Watzek, G., 1995. Incidence and suggested surgical management of septa in sinus-lift procedures. Int J Oral Maxillofac Implants. 10, 462–465.

Wen, S.C., Chan, H.L., Wang, H.L., 2013. Classification and management of antral septa for maxillary sinus augmentation. Int J Periodontics Restorative Dent. 33, 509-517.

Yang, H. M., Bae, H. E., Won, S. Y., Hu, K. S., Song, W. C., Paik, D. J., Kim, H. J., 2009. The buccofacial wall of maxillary sinus: an anatomical consideration for sinus augmentation. Clin Implant Dent Relat Res. 11, 2–6.

Yang, S.M., Park, S.I., Kye, S.B., Shin, S.Y., 2012. Computed tomographic assessment of maxillary sinus wall thickness in edentulous patients. J Oral Rehabil. 39, 421-428.

Zijderveld, S.A., Van den Bergh, J.P., Schulten, E.A., ten Bruggenkate C.M., 2008. Anatomical and surgical findings and complications in 100 consecutive maxillary sinus floor elevation procedures. J Oral Maxillofac Surg. 66, 1426-1438.

FIGURES LEGEND

Fig. 1. Overview of a CBCT Scan performed with a radiological guide: (a) image of the radiological marks on an image of the coronal plane; (b,c,d) image of radiological marks on sagittal plane corresponding to different slices.
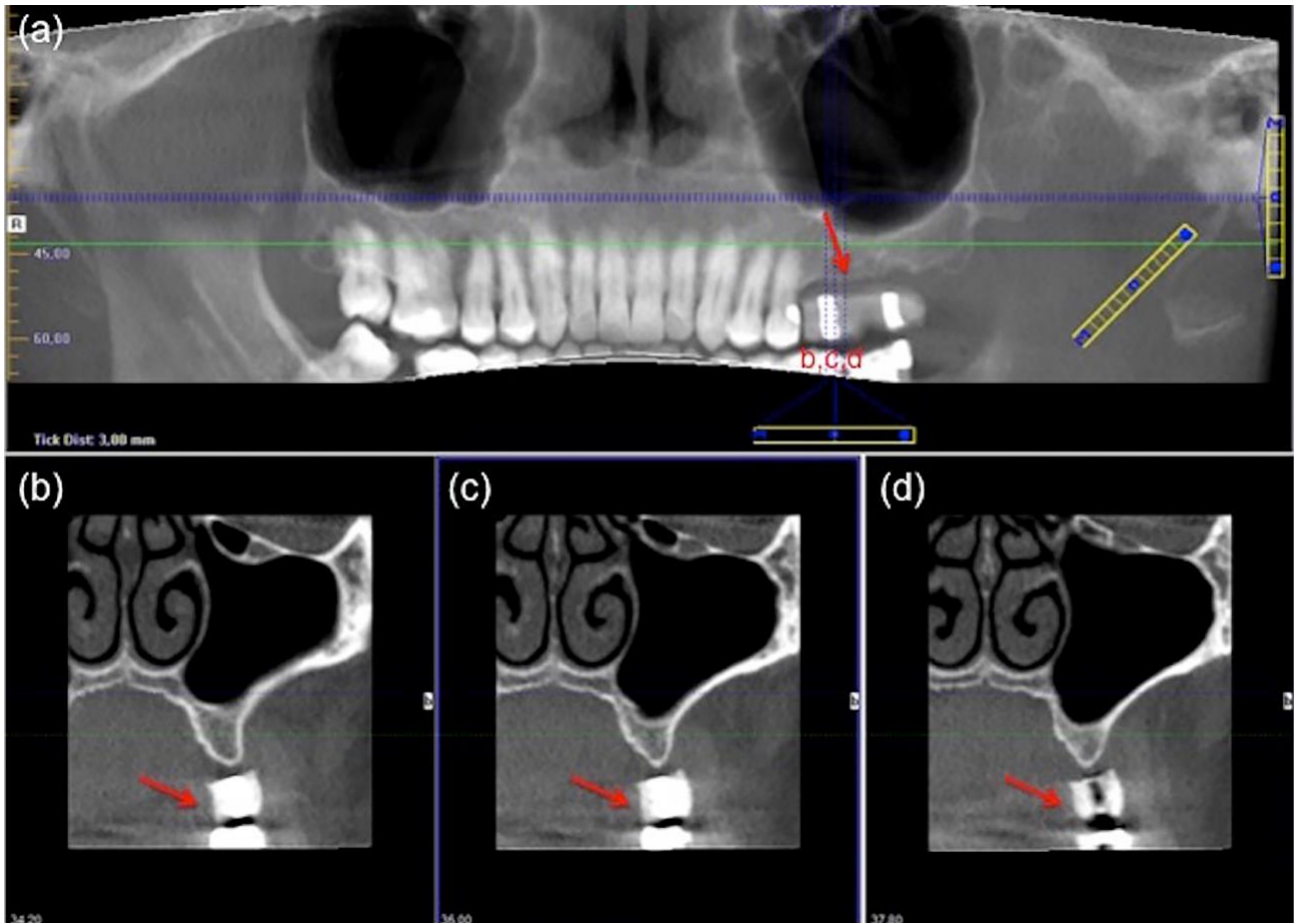
Fig. 2.

1) Measurements of residual ridge height (RRH); 2) width (RRW); 3) & 4) and maxillary sinus angle (MSA) measurements in the sagittal plane.
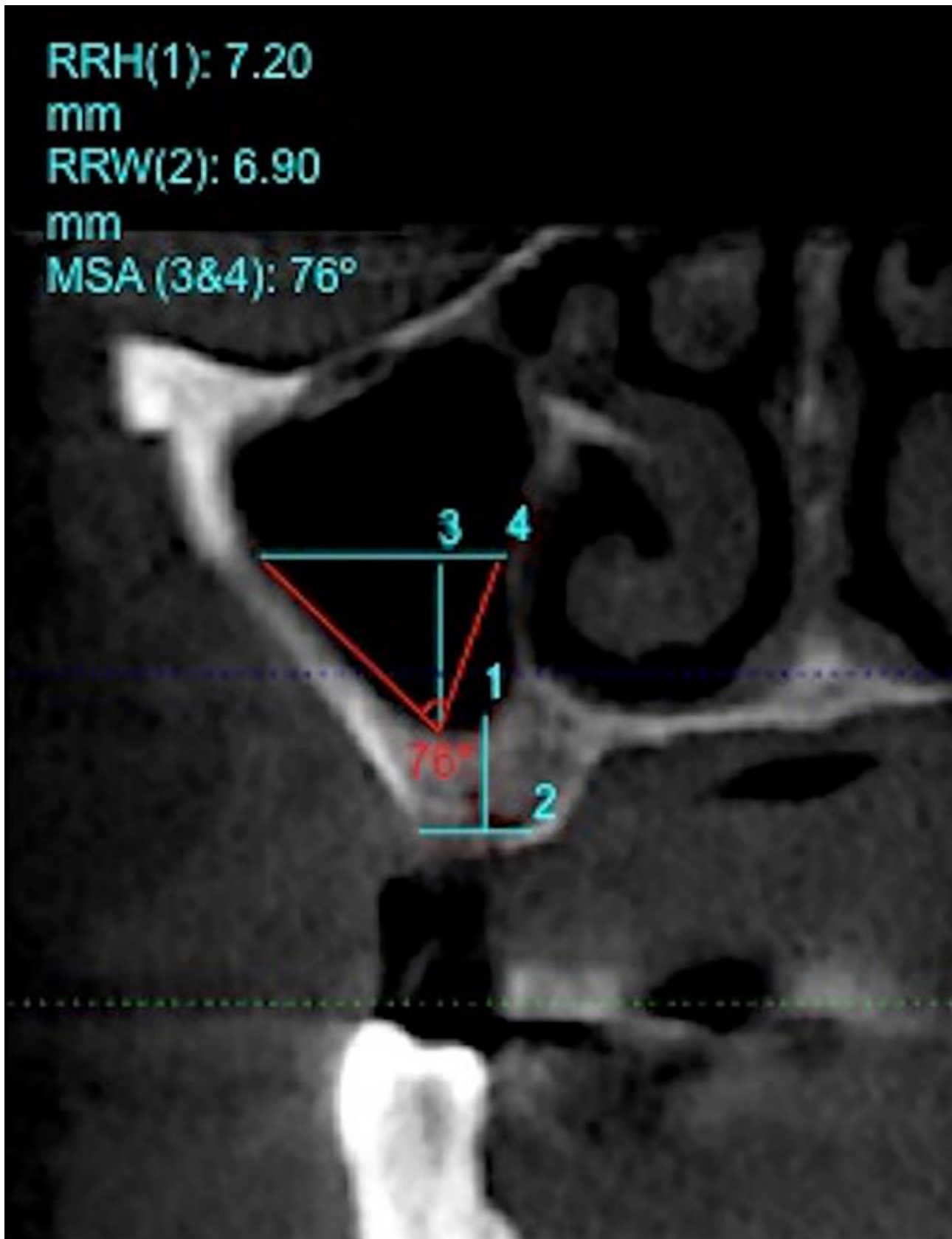
Fig. 3. Image of the posterior superior alveolar artery (PSAA): (a,c,d,e,f) sagittal slices; (b) measurement of the distance from the lower border of the artery (PSAA) to the alveolar crest, in the sagittal plane.
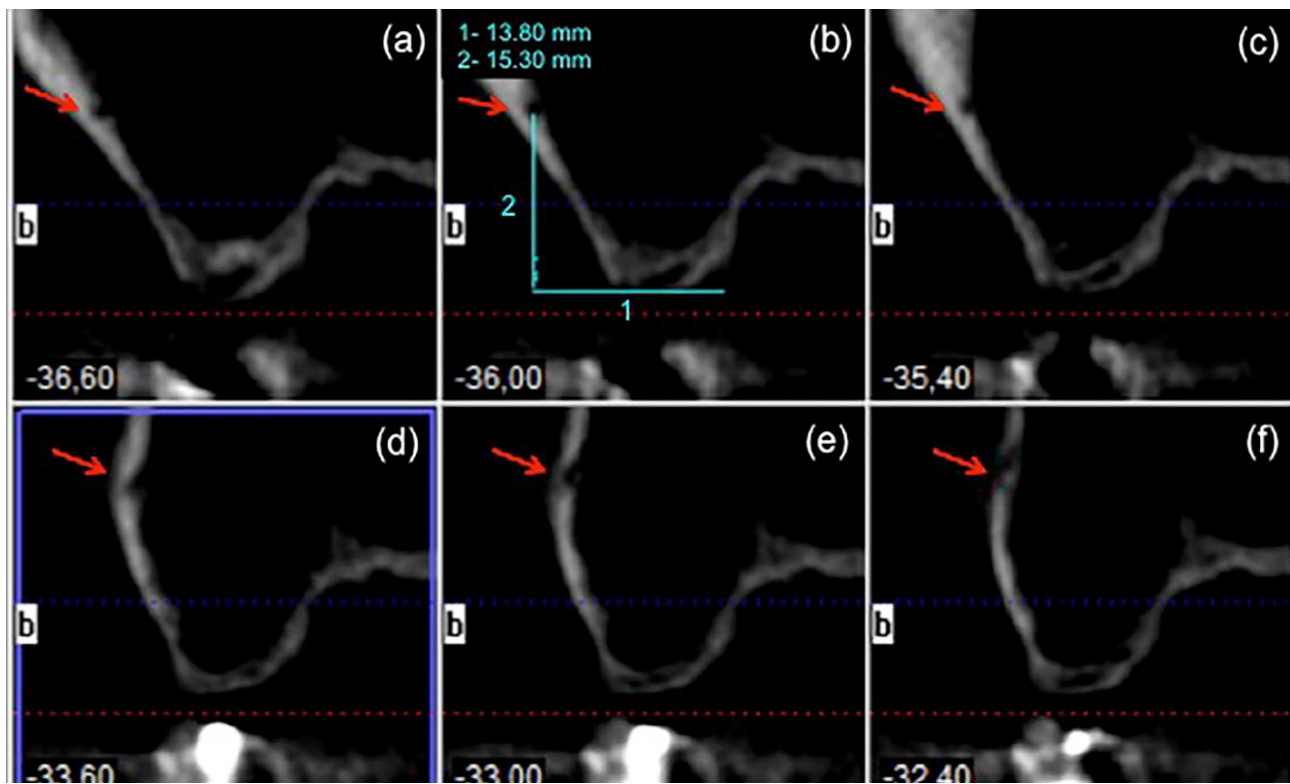
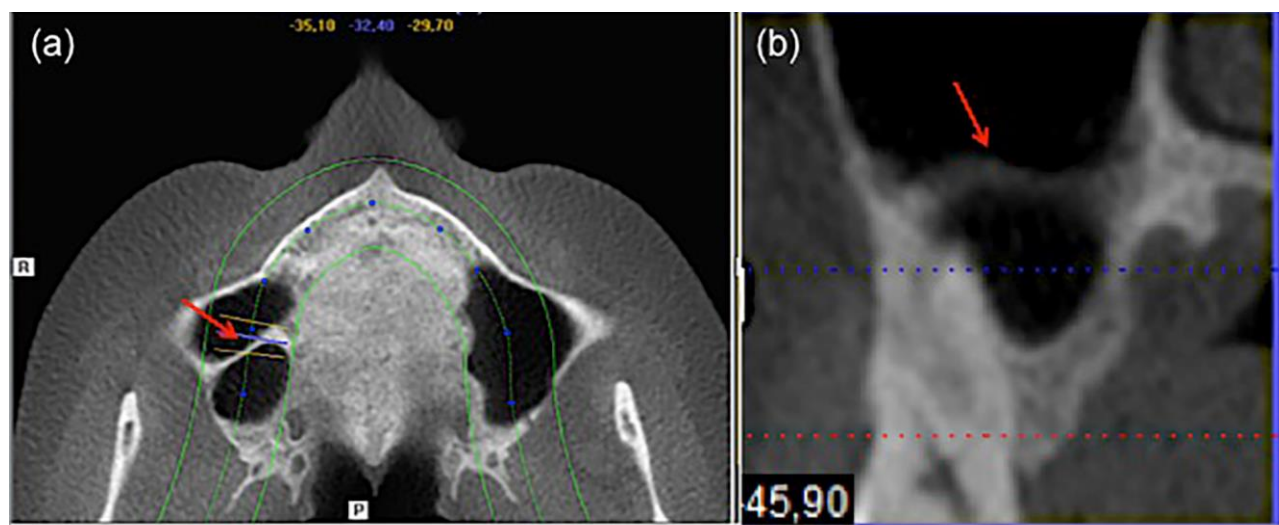Fig. 4. Overview of transversal (bucco-palatal) septum in CBCT scan: (a) axial view; (b) sagittal view.

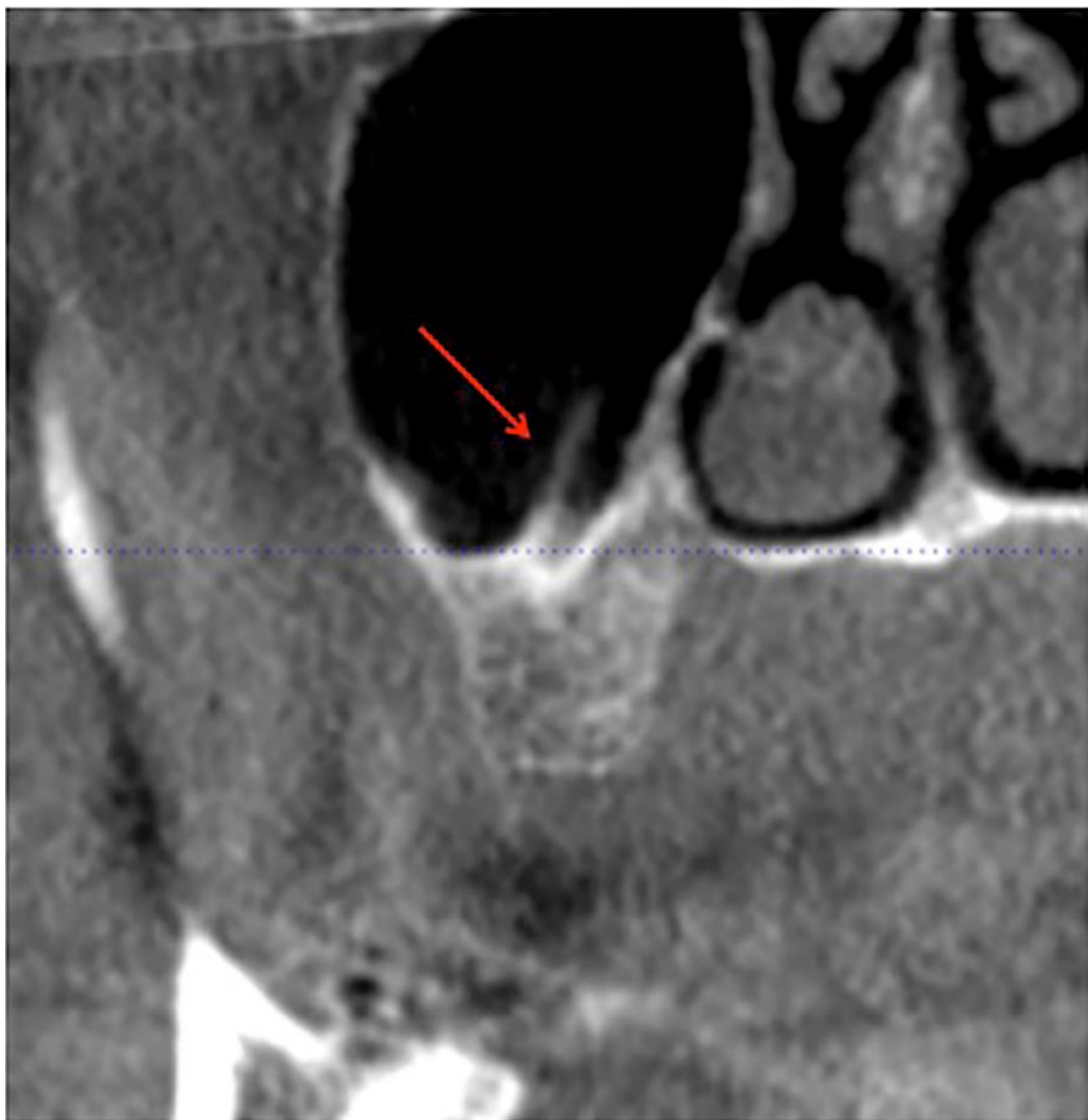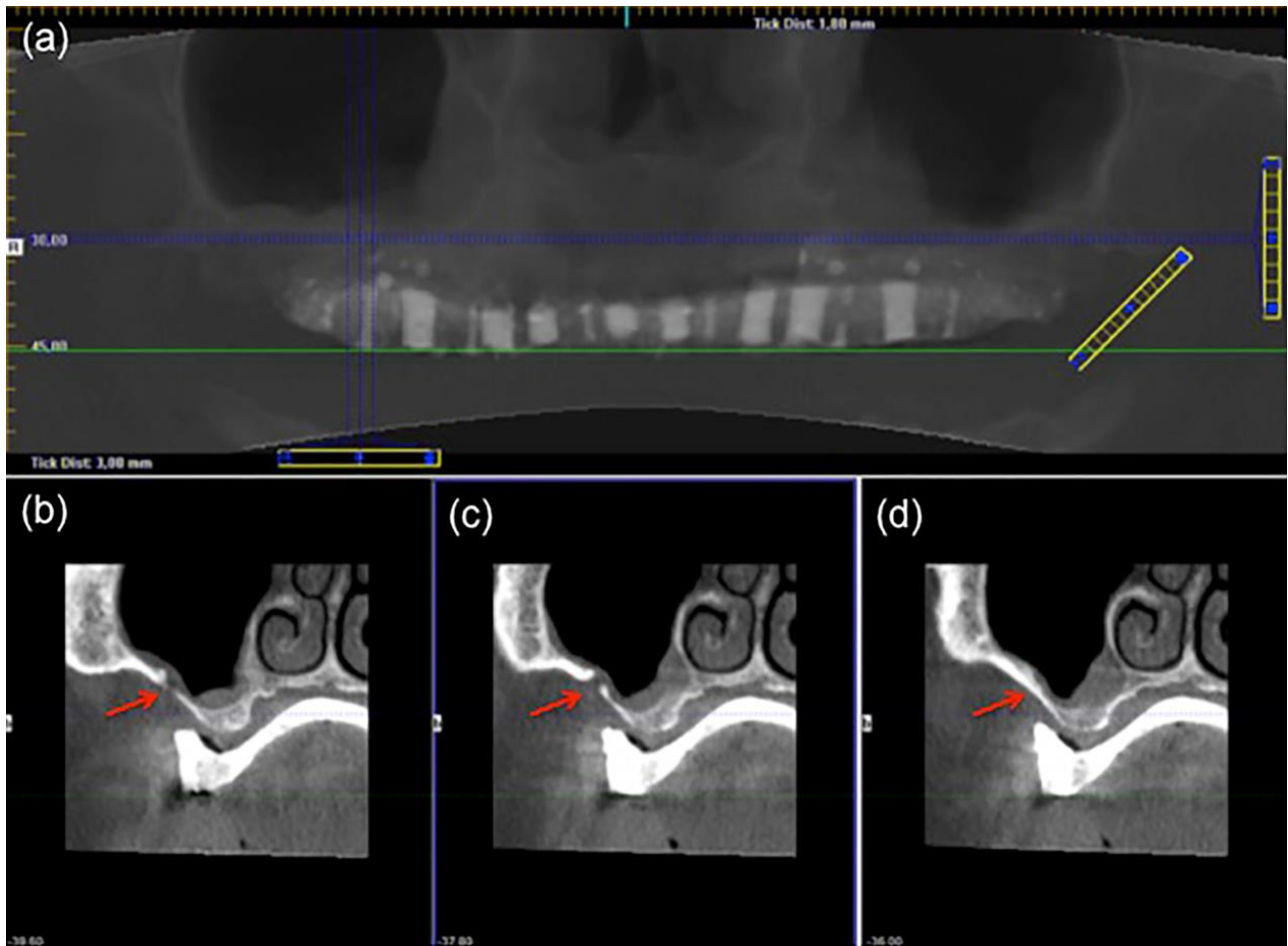Fig. 5. Sagittal view of a sagittal (mesio-distal) septum.

Fig. 6. CBCT scan of an intraosseous PSAA through the lateral wall of the maxillary sinus, in the first molar region: (a) coronal plane; (b,c,d,) sagittal slices.

TABLES LEGEND

Table 1: The distribution of residual ridge height (RRH) and wide (RRW), bone density (BD) and maxillary sinus angle (MSA) according to maxillary region.

Observer	RRH (mm)			RRW (mm)			BD (HU)	MSA (°)
	2PM	1M	2M	2PM	1M	2M	1M	1M
1	8.66±3.95	4.90±2.28	5.26±2.13	6.72±2.69	6.87±2.65	7.09±2.8	330.93±211.02	73.39± 15.23
2	9.33±4.64	4.58±2.19	4.54±2.16	6.29±2.35	6.74±2.76	7.48±3.02	325.27±186.07	73.65± 14.98
p- value	0.1679	0.0900	0.0784	0.0958	0.5294	0.2663	0.7116	0.6247

Data expressed as mean ± standard deviation. Level of significance was set at *P*-value <0.05.

Table 2: Lateral Wall thickness (LWT) and Schneiderian membrane thickness (MT) at 1st molar region.

Observer	LWT (mm)	MT		
	1M	1M (mm)	≤3(%)	>3(%)
1	1.95±0.98	1.82±1.59	72.90	27.10
2	1.76±0.56	1.64±1.09	73.83	26.17
p- value	0.1	0.0845		
Kappa			0.928 (Very Good)	

Data expressed as mean ± standard deviation. Frequency of MT ≤ 3mm ("Normal") and > 3mm (" Pathological"), expressed as percentage. Comparison of intraobserver agreement, level of significance was set at *P*-value <0.05 for quantitative variables and Kappa-Index analysis for qualitative variables.

Table 3: Prevalence, height and location of sinus septa according to orientation.

Observer	Bucco-palatal Septa			Sagittal Septa		
	Frequency (%)	Height (mm)	Location	Frequency (%)	Height (mm)	Location
1	20.56%	13.11±3.82	(2PM) 13.64%	3.74%	12.24±1.25	(2PM) 50%
			(1M) 22.73%			(1M) 25%
			(2M) 40.91%			(2M) 0%
			(3M) 22.73%			(3M) 25%
2	19.63%	12.73±4.21	(2PM) 9.52%	3.74%	10.58±6.17	(2PM) 25%
			(1M) 14.29%			(1M) 25%
			(2M) 47.62%			(2M) 50%
			(3M) 28.57%			(3M) 0%
p-value		0.3792				
Kappa	0.738 (Good)		0.833 (Very Good)	-0.039 (Poor)		

Comparison of intraobserver agreement, level of significance was set at *P*-value <0.05 for quantitative variables and Kappa-Index analysis for qualitative variables.

Table 4: Incidence, location and height of posterior superior alveolar artery (PSAA).

Observer	Frequency (%)	Location	Distance (mm)	Position	Diameter
		Posterior Superior Alveolar Artery (PAAS)			
1	48.60%	(2PM) 19.23%	13.15±3.71	(*IN*) 53.85%	(<1 mm) 36.54%
		(1M) 46.15%		(*INTRA*) 38.46%	(1-2 mm) 28.85%
		(2M) 28.85%		(*OUT*) 7.69%	(>2 mm) 34.62%
		(3M) 5.77%			
2	49.53%	(2PM) 18.87%	13.93±3.68	(*IN*) 32.08%	(<1 mm) 60.38%
		(1M) 45.28%		(*INTRA*) 64.15%	(1-2 mm) 35.85%
		(2M) 30.19%		(*OUT*) 3.77%	(>2 mm) 3.77%
		(3M) 5.66%			
p- value			0.5273		
Kappa	0.682 (Good)	0.311 (Weak)		0.404 (Moderate)	0.145 (Poor)

(Data expressed as mean ± standard deviation), frequency of position and distribution of diameter in the three categories. *IN*, position of the artery below the membrane. *INTRA*, position of the artery intraosseous. *OUT*, on the outer cortex of the lateral sinus wall.

Comparison of intraobserver agreement, level of significance was set at *P*-value <0.05 for quantitative variables and Kappa-Index analysis for qualitative variables.